Gas-Liquid Displacement Method for Estimating Membrane Pore-Size Distributions

P. Shao, R. Y. M. Huang, X. Feng, and W. Anderson
Dept. of Chemical Engineering, University of Waterloo, Waterloo, Ontario, Canada N2L 3G1

A gas-liquid displacement method is investigated for characterizing pore-size distributions of microfiltration (MF) membranes. The complexities of using gas as displacing fluid are analyzed in terms of the gas transport regimes involved, showing that slip flow features gas transport in MF membranes, and Knudsen diffusion can be effectively suppressed by an appropriate selection of the pore-filling liquid. A universal mathematical model for evaluating pore-size distributions is developed based on the fundamental equation governing slip flow. An approximate model is also presented where only the Hagen-Poiseuille regime is considered. The pore-size distributions of two MF membranes are evaluated using the universal and the approximate models, respectively. It is found that the approximate model overestimates the probability of the larger pore (relative to the peak pore) and underestimates the probability of the smaller pore. It is recommended that the universal model be used if no priori analyses on gas transport regimes is carried out. © 2004 American Institute of Chemical Engineers *AIChE J,* 50: 557–565, 2004
Keywords: skip flow, Knudsen diffusion, Hagen-Poiseuille Flow, pore-size distribution, surface tension

Introduction

Microfiltration membranes (MF) can be made highly porous, and with asymmetric structures through some clever manipulations implemented in the process of preparation (Bottino et al., 1991; Frommer and Messalem, 1973). As such, they demonstrate very low transport resistance, and found wide applications in many industries (such as food, pharmaceutical, and electronics) as a viable substitute for the traditional porous media (such as ultrafine glass fibers and nonwoven fabrics) for separation and purification applications. Selection of a MF membrane for a specific application requires a good understanding on its permeation flux, porosity, bubble point, mean pore size, and pore-size distribution. The knowledge of pore-size distribution is more important to the success of the application, since the selection of a membrane based on its mean pore size does not guarantee the expected separation or rejection performance. For example, the perfect removal of bacteria (such as 0.22 μm) from processing streams in the pharmaceutical industry is a must; a membrane with a nominal pore size of 0.22 μm does not necessarily satisfy this criterion, depending on the fraction of the larger pores relative to the nominal pore size present in the membrane. For the assurance of process quality, prior knowledge on pore-size distribution of the selected membrane is critically important.

Many methods can be used for estimating pore-size distributions (Kullkarni et al., 1992; Mulder, 1991; Smith et al., 1977; McEaney et al., 1988). Mercury intrusion is typically employed for the evaluation of porous media (such as supports for catalysts and adsorbents) to disclose such information as specific pore volume and specific internal surface area. As it is known that mercury intrusion usually involves very high pressures (Honold and Skau, 1954; Lowell et al., 1987), which only strong porous media can withstand, its application for evaluating MF membranes is, thus, quite limited. Capillary condensation based on Kelvin equation is also employed as a principle for evaluating pore-size distribution. It is well known that significant condensation of inert gases (such as N_2, He) occurs only in pores of very fine diameters (Dollimore and Heal, 1964); this method is thus mainly used to evaluate the pore-size

Correspondence concerning this article should be addressed to R. Y. M. Huang at ryhuang@uwaterloo.ca.

Table 1. Interfacial Tensions of some Liquid Pairs at 20°C

System	*Interfacial Tension (mJ/m^2)
Water-butanol	1.8
Water-butanol-methanol: 25/15/7 (v:v)	0.35

*Data from literature (Jakob and Koros, 1997).

distributions of ultrafiltration and nanofiltration membranes. In addition, both these methods are based on equilibrium (either hydrodynamic or thermodynamic), and, thus, tell no difference between the through-pores and the dead-end pores. It is well known that dead-end pores are intrinsically present in membrane structures, however, they contribute nothing to the transport properties of membranes. As a result, both methods cannot provide accurate information on pore-size distributions of membranes. Based on this understanding, a common insight is reached that dynamic methods (Jakobs and Koros, 1997) should be selected for characterizing the pore-size distributions of membranes.

Liquid-liquid (l-l) displacement is one of the dynamic techniques for evaluating pore-size distributions (Kamide and Manabe, 1980; Kesting, 1985). All the pores of a to be tested membrane are, at first, filled with a wetting liquid, which can penetrate into the pores automatically due to the favorable capillary force; another liquid is then forced into the pores to progressively expel the former one. By monitoring the transmembrane pressure dependence of the flux of the displacing liquid, the pore-size distribution can be figured out.

Water/butanol is a typically used liquid pair. The interfacial tension of water-butanol is 1.7 mJ/m^2 as shown in Table 1, which is found to be suitable for characterizing mesopores (2 $\sim$ 50 nm). For analyzing pore sizes larger than 50 nm (typically present in MF membranes), the interfacial tensions of the typical liquid pairs are not high enough to produce a wide range of bursting pressure, over which the progressive (l-l) displacement is carried out. As a result, the available pressure increment (0.1 psi or even less) cannot be made large enough to eliminate unnecessary reading errors, and, most importantly, the operability of the progressive (l-l) displacement by means of increasing pressure in that small increment is unduly reduced.

Surface tensions of gas-liquid (g-l) systems (17 $\sim$ 73 mJ/m^2), as shown in Table 2, are much higher than the typical interfacial tensions (1 $\sim$ 3 mJ/m^2) of (l-l) systems. Displacement of the liquid in membrane pores using an inert gas (such as nitrogen and air) instead of a liquid can, thus, overcome the above-mentioned defect. However, it should be noted that the mass transport in membrane pores can be complicated when gas is used as the displacing fluid, since the mechanism of gas transport through capillary pores depends on the ratio of the pore size to the mean free path of the displacing gas. It is generally accepted that the Hagen-Poiseuille regime dominates gas transport in a pore when the pore size is much larger than the mean free path of the displacing gas. On the other hand, when the mean free path is much larger than the pore size, Knudsen diffusion dominates the transport. In the transitional region where the pore size is comparable to the mean free path, viscous slip flow takes place (Scott and Dullien, 1962). In this case, the assumption that the molecules on the pore wall are stationary, as held in Hagen-Poiseuille regime, is no longer valid due to the significant presence of Knudsen diffusion.

An empirical approach was adopted by earlier researchers in the investigation of gas transport through capillary pores in transitional region. Evans and Watson (1962) included both Hagen-Poiseuille flow and Knudsen diffusion in their transport equation with two disposable parameters by

$$J = A + B\bar{p}/\eta \tag{1}$$

where parameter A represents the contribution of Knudsen diffusion to the total permeation rate of the gas in slip flow, B is a proportionality constant related to the contribution of Poiseuille flow, and η is the viscosity of the gas. The two adjustable parameters A and B in Eq. 1 can be estimated by fitting the equation with experimental data. Although Eq. 1 agrees with experimental data very well, it cannot be used as a fundamental equation for estimating pore-size distributions, since no priori correlation of the parameters A and B to Knudsen diffusion and Hagen-Poiseuille flow was theoretically formulated.

Based on gas kinetic theory, Otani et al. (1965) and Wakao et al. (1965) derived an equation governing gas transport in transition region in a single pore, as shown in Eq. 2, and it was found that the theoretical predictions were in good agreement with experimental data

$$N^{\text{transition}} = \frac{\Delta p}{RTL}\left[\phi D_K + (1-\phi)\left(\frac{\pi D_K}{4} + \frac{r^2\bar{p}}{8\eta}\right)\right] \tag{2}$$

$$\phi = \frac{\text{wall collision frequency}}{\text{total collision frequency}} = \frac{1}{1+\dfrac{2r}{\lambda}} \tag{3}$$

where R is universal gas constant, T is absolute temperature, L is the length of the assumed cylindrical circular pore, r is the radius of the assumed cylindrical circular pore, $\bar{p}$ is the average of the pressures at both ends of a pore, η is the viscosity of the gas, D_K is Knudsen diffusion coefficient, ϕ is the fraction of the collisions leading to Knudsen diffusion, r is pore radius, and λ is the mean free path of the gas. Three fundamental regimes are involved in transitional flow, which are the Hagen-Poiseuille regime represented by the term of $(r^2\bar{p}/8\eta)$ in Eq. 2, Knudsen diffusion regime by ϕD_K, and slip flow regime by $(1-\phi)(\pi D_K/4)$. Although this important equation was first derived in 1965, no reports of its applications were found in literature as a fundamental equation for characterizing pore-

Table 2. Surface Tensions of some Liquids at 20°C

System	*Surface Tension (mJ/m^2)
Water-air	72.8
Glycerol-air	63.4
Methanol	22.6
Ethanol-air	22.8
1-Propanol-air	23.8
2-Propanol-air	21.7
Benzene-air	28.9
n-Hexane-air	18.4
Diethyl ether-air	17.0

*Data from *Handbook of Chemistry and Physics,* The Chemical Rubber Co. 43rd Edition, Cleveland, OH.

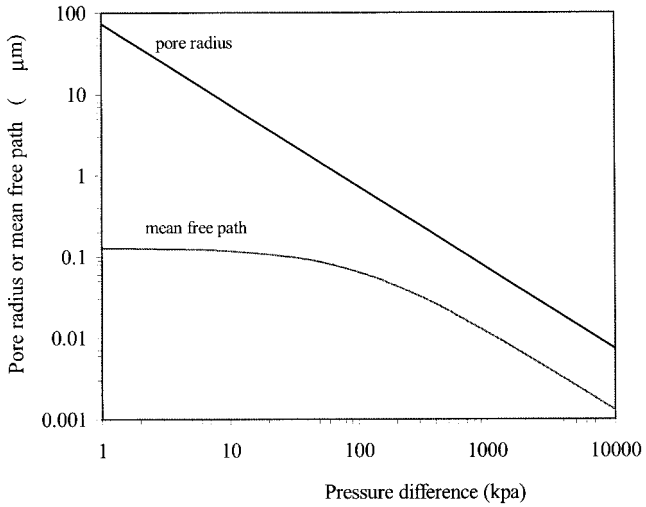

Figure 1. Plot of pore radius and mean free path vs. pressure difference.

size distributions of porous media over the past decades. As a matter of fact, empirical treatments were very often practiced in previous work (Pereira and Peinemann, 1992; Schofield et al., 1990).

The gas-liquid displacement method is attempted in this work for evaluating the pore-size distributions of MF membranes. Due to the diversity of gas transport regimes involved in capillary flows, a theoretical analysis is carried out. The influences of the factors determining the transport regime are elucidated, revealing that the gas transport regime in the pores is determined not only by the magnitude of the pore sizes, but also by the magnitude of the surface tension of the selected pore-filling liquid. Generally speaking, gas transport in MF membranes (0.1 $\sim$ 10 μm) is dominated by slip flow. A universal model for estimating pore-size distributions was developed based on Eq. 2. Knudsen diffusion can be suppressed by a proper selection of the pore-filling liquid that must have sufficiently high surface tension (such as that of water) and a very small contact angle (close to zero). In this situation, the slip flow can be treated as pure viscous flow. An approximated model based on pure viscous flow regime is also presented. The pore sizes of two MF membranes were analyzed with respect to different versions of pore-size distributions (such as the incremental distribution, the differential distribution) using both the universal, and the approximated models.

Theoretical

Gas transport regimes in the opened pores

According to Cartor equation (Bechhold et al., 1931), as expressed in Eq. 4, in order to force a pore-filling liquid out of a pore of radius r, a minimum gas pressure difference should be applied to counteract the capillary force caused by the interface tension of the liquid

$$\Delta p = \frac{2\gamma \cos\theta}{r} \tag{4}$$

where γ is the surface tension of the liquid, θ is the contact angle of the liquid on the inner surface of the pore, and r is the radius of the circular cylindrical pore. Equation 4 suggests that a smaller liquid-filled pore can be opened with an increased gas pressure difference.

According to gas kinetic theory (Present, 1958; Mason and Malinauskas, 1983), the mean free path of a gas can be expressed as

$$\lambda = \frac{1}{\sqrt{2}\ \pi\rho^2 n} \tag{5}$$

where ρ is diameter of a gas molecule and n is the number of gas molecules in unit volume, which can be estimated by using the state equation for ideal gases by

$$n = \frac{(p + p_0)}{kT} \tag{6}$$

where p, p_0 are gas pressures indicated by gauge (equivalent to Δp in Eq. 4), and the atmospheric pressure, respectively; k is the Boltzmann constant. Substitution of Eq. 6 into Eq. 5 yields

$$\lambda = \frac{kT}{\sqrt{2}\ \pi\rho^2(p + p_0)} \tag{7}$$

In the case of using water (surface tension at 20°C: 72.8 mJ/m^2) as the pore filling liquid and nitrogen as the displacing gas, the transmembrane pressure dependence of the radius of the pore being opened and the mean free path of the displacing gas in the pore is plotted in Figure 1. It can be found that the radius of the pore currently opened is always larger than the current mean free path of the displacing gas. It is known that the ratio of the pore radius to mean free path is more important, by which the dominating gas transport regime can be judged. With this ratio, the fraction of Knudsen diffusion (Φ) can be estimated using Eq. 2, which is illustrated in Figure 2. For general

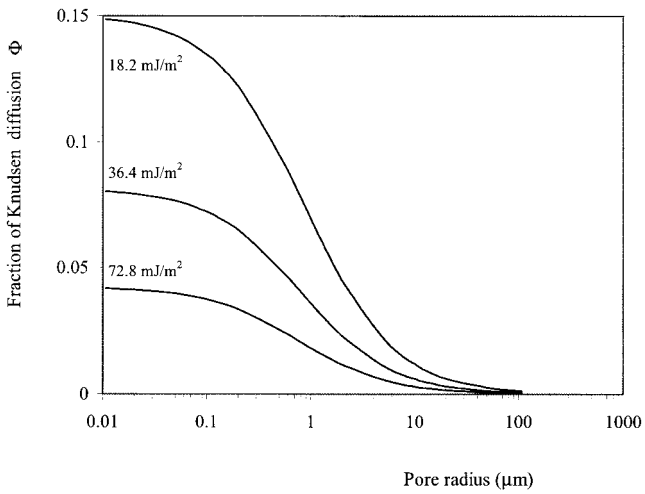

Figure 2. Dependence of the fraction of Knudsen diffusion in slip flow on pore radius and effective surface tension of the selected liquid.

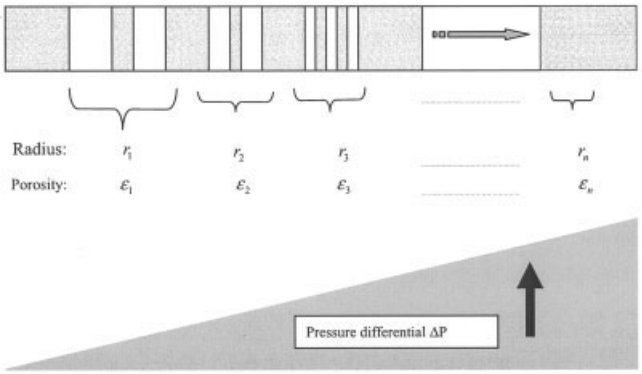

Figure 3. Grouped pores and the corresponding opening pressure.

purposes, the effective surface tension ($\gamma \cos \theta$) of the selected liquid is also considered as an affecting parameter in Figure 2. Clearly, when the effective surface tension of the pore-filling liquid is 72.8 mJ/m^2 (equal to the surface tension of water at 20°C), the fraction of Knudsen diffusion is always less than 5%. If the selected liquid has a smaller surface tension (such as 36.4, 18.2 mJ/m^2), as shown in Figure 2, the fractions of Knudsen diffusion in the pores are always significant and its contribution should, therefore, always be considered. Figure 2 also suggests that Knudsen diffusion in the opened pores can be effectively suppressed by selecting a right pore-filling liquid having an effective surface tension no less than 72.8 mJ/m^2. As a matter of fact, this criterion that the effective surface tension should be larger than 72.8 mJ/m^2 is very hard to fulfill, since most liquids have smaller surface tensions than that of water. As a result, gas transport in MF membranes can be generally characterized by slip flow, and Eq. 2 should be used as the fundamental equation for estimating pore-size distributions of the membranes. Otherwise, inaccurate information can be resulted in.

Mathematical model

For the sake of simplicity, pores in a membrane are grouped such that all those of comparable sizes are put together, as shown in Figure 3. Experimentally, the transmembrane pressure can be increased little by little in a progressive manner. It can, thus, be reasonably assumed that all the pores that opened as the result of a small increment in gas pressure are of the same size, which is represented by r_i, and the porosity of this group of pores is represented by ε_i.

The permeation rate of the displacing gas through this group of cylindrical circular pores in slip flow regime can be obtained from Eq. 2

$$J_i = \frac{\varepsilon_i}{RTL}\left[\phi_i D_K + (1-\phi_i)\left(\frac{\pi}{4} D_K + \frac{r_i^2}{8\eta}\overline{p_i}\right)\right] \tag{8}$$

where D_K is the Knudsen diffusion coefficient, and, according to gas kinetic theory, it can be written as

$$D_K = \frac{2r_i}{3}\sqrt{\frac{8RT}{\pi M}} \tag{9}$$

ϕ_i is the contribution of Knudsen diffusion in this group of pores, which can be written as

$$\phi_i = \frac{1}{1 + 2r_i/\lambda_i} \tag{10}$$

Now, it assumed that $N + 1$ groups of pores of varying pore sizes have been opened, and the $(N + 1)^{\text{th}}$ group is the currently opened group. The total permeation rate (also called as current permeation rate in this article) of the displacing gas through $(N + 1)$ groups of pores can be written as

$$J^C = \sum_1^N \frac{\varepsilon_i}{RTL}\left[\phi_i D_K + (1-\phi_i)\left(\frac{\pi}{4} D_K + \frac{r_i^2}{8\eta}\overline{p_{N+1}}\right)\right] + \frac{\varepsilon_{N+1}}{RTL}\left[\phi_{N+1} D_K + (1-\phi_{N+1})\left(\frac{\pi}{4} D_K + \frac{r_{N+1}^2}{8\eta}\overline{p_{N+1}}\right)\right] \tag{11}$$

where superscript C means "current." It is known that the mean free path of the displacing gas is dependent on the current displacing pressure, which increases progressively in the experiment. Therefore, the fraction of Knudsen diffusion (ϕ_i) in a random group of the opened pores is also dependent on the current displacing pressure, which can be universally expressed as

$$\phi_i = \frac{1}{1 + \dfrac{2r_i}{\lambda_{N+1}}} \tag{12}$$

$$i = 1, 2, \ldots, N, N+1$$

Now that the radius and the porosity of each group of the opened pores are estimated, and the radius of the currently opened pores can also be estimated by Eq. 4, the porosity of the currently opened pores can thus be determined as follows

$$\varepsilon_{N+1} = \frac{J^C - \sum_1^N \dfrac{\varepsilon_i}{RTL}\left[\phi_i D_K + (1-\phi_i)\left(\dfrac{\pi}{4} D_K + \dfrac{r_i^2}{8\eta}\overline{p_{N+1}}\right)\right]}{\dfrac{1}{RTL}\left[\phi_{N+1} D_K + (1-\phi_{N+1})\left(\dfrac{\pi}{4} D_K + \dfrac{r_{N+1}^2}{8\eta}\overline{p_{N+1}}\right)\right]} \tag{13}$$

The initial (the first opened pore group) porosity ε_1 can be obtained by assuming the summation term in the nominator of Eq. 13 to be zero. It should be pointed out that such obtained porosity contains the length L of the assumed cylindrical circular pore, which can be mathematically expressed as $\varepsilon_i = c_i{*}L$. However, according to the following defined pore-size distributions (see Eqs. 16 and 17), and/or the dimensionless treatment (see Eq. 19), the length L can be mathematically eliminated. Therefore, the knowledge of the length L of the assumed cylindrical pores of the membrane is not necessary.

Note that one simpler equation can be obtained by assuming $\phi = 0$, meaning that only the Hagen-Poiseuille regime occurs

to the membrane. This assumption is valid when the pore sizes of the membrane are quite large (such as >5 μm), or when a right pore-filling liquid is selected as discussed previously. In this situation, Eq. 13 is reduced as

$$\varepsilon_{N+1} = \frac{8RT\eta L * \dfrac{J_C}{p_{N+1}} - \sum_{1}^{N} \varepsilon_i r_i^2}{r_{N+1}^2} \tag{14}$$

Pure Knudsen diffusion ($\phi = 1$) in MF membranes is scarcely possible; therefore, it is not considered in model formulation.

So far, if all the available pores in a membrane have been opened, the total porosity ε_t of a membrane can be obtained by adding the porosity of each pore group ε_i

$$\varepsilon_t = \sum \varepsilon_i \tag{15}$$

Based on these original data, the pore-size distribution of the membrane can be constructed. As a matter of fact, many versions of pore-size distributions can be found in literatures (Schofield et al., 1990; Hernandez et al., 1996; Meyer and Klobes, 1999), which can be classified into three categories, incremental distribution, cumulative distribution, and differential distribution. The incremental and cumulative distributions are self-evident, and the incremental pore-size distribution is hereby defined as $f(r_i) = (1/\varepsilon_t)\sum_{1}^{i}\varepsilon_i$.

For convenience in description, this distribution is donated as $(\varepsilon - r)$ in symbol. In some literatures (Kang et al., 2002; Hernandez et al., 1996) the number of pore was used to define the pore-size distributions, but, for the ease in the applications of such information, the porosity is used as a substitute in this work. Accordingly, the cumulative distribution is defined as $f(r_i) = (1/\varepsilon_t) \sum_{1}^{i} \varepsilon_i$. It should be noted that this definition is different from the conventional one in that it represents the sum of the fractions of porosity of all the pores larger than r_i in pore size, since, in progressive displacement experiment, the larger pores are opened preferentially.

The differential distribution function $f_a(r)$ in terms of porosity is defined as

$$f_a(r_i) = \frac{1}{\varepsilon_t}\frac{d\varepsilon}{dr} = \frac{1}{\varepsilon_t} * \frac{\varepsilon_i}{(r_{i-1} - r_i)} \tag{16}$$

For convenience in description, this distribution is donated by $[(d\varepsilon/dr) - -r]$ in symbol.

The differential pore-size distribution in terms of flux contribution is defined as

$$f_f(r_i) = \frac{1}{\sum \varepsilon_i r_i^2} * \frac{\varepsilon_i}{(r_{i-1} - r_i)} \tag{17}$$

and, accordingly, it is donated by $[(d\varepsilon r^2/dr) - -r]$ in symbol.

Again, for the convenience in comparing different versions of pore-size distributions, all the defined distribution functions are normalized using the following dimensionless treatment

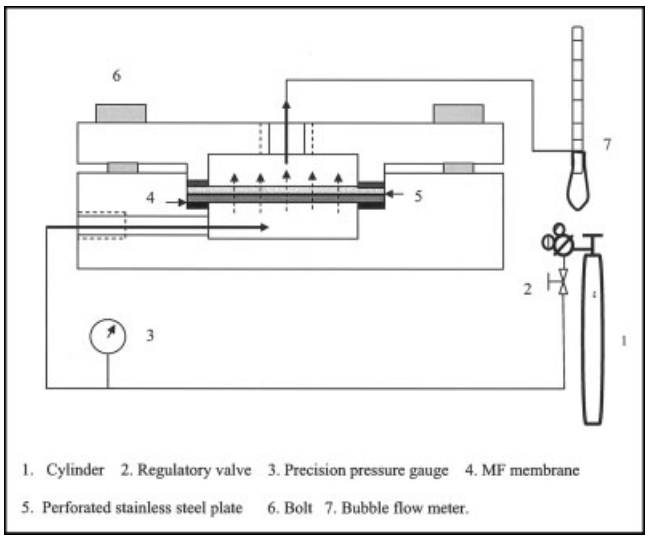

Figure 4. Setup for evaluating the pore-size distributions of MF membranes.

$$P(r_i) = \frac{f(r_i)}{\sum f(r_i)} \tag{18}$$

It should be pointed out that the mathematical treatment as shown in Eq. 18 does not change the characteristics in pore-size distributions, however, it makes the comparison friendly.

Experimental

Preparation of two types of MF membranes

10 g sulfonated poly(ether ether ketone) having a degree of sulfonation (DS) of 67% (prepared in our lab) was dissolved in 85 mL N-methyl pyrrolidone (NMP) to prepare the polymer solution, in which 5 mL ethanol was added as additive. The obtained homogeneous casting solution was then spreaded on the surface of nonwoven fabric, and the cast polymer solution films were precipitated in two aqueous coagulants containing different isopropanol contents (20 and 80% IPA) attempting to obtain porous membranes with different porosity and pore-size distributions. The precipitated membranes were then transferred to a water bath to extract the residual solvent for a week. The solvent-depleted membranes were cleaned thoroughly with deionized (DI) water before being dried in an air-drying chamber.

Progressive gas-liquid displacement experiment

The dried membrane was cut into disk form with a diameter of 20 mm. Make sure that all the operations involved in the preparation and the tests of the membrane samples cause no contamination in the membrane surfaces. The round membrane sample was first immersed into a water (DI) flask to get fully wetted before being mounted into the test cell, as shown in Figure 4. Thin flat sheet O ring seals were used on both sides of the membrane, and a finely perforated stainless steel plate with a pore size of 1 mm was put on the surface of the thin O ring to prevent deformation of the membrane caused by the high transmembrane pressure. The experiment was carried out

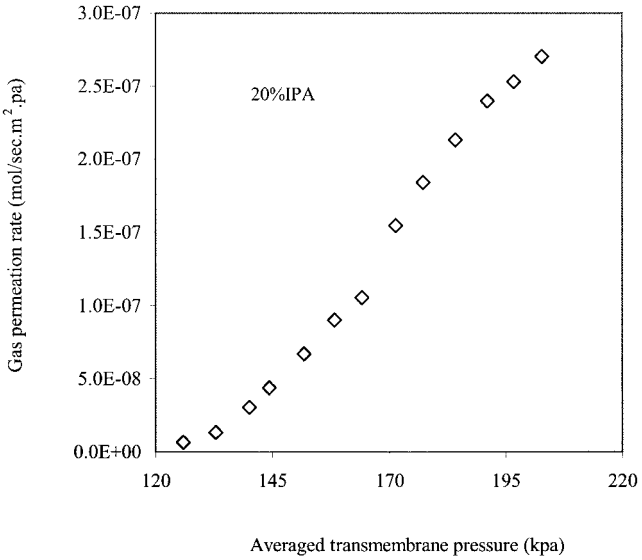

Figure 5. Progressive gas permeation rate of membrane A vs. the averaged pressure.

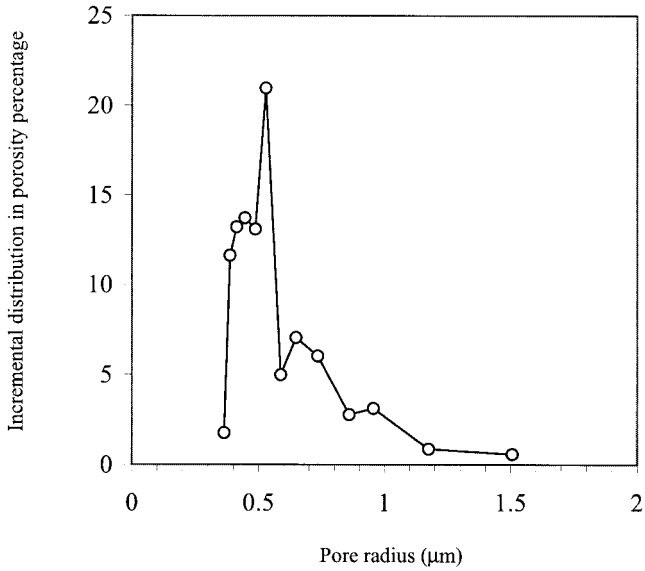

Figure 7. Incremental pore-size distribution of membrane A.

at 20°C with nitrogen used as the displacing gas. The contact angle of DI water on the surface of the sulfonated poly(ether ether ketone) (67% DS) was 58.2 degrees as reported in our previous paper (Huang et al., 2001). The gas pressure was increased progressively with an increment of about 2–3 psi. The permeating gas was collected and measured with a bubble flowmeter. The gas permeation rate of the membrane is defined as follows

$$J = \frac{V}{A\Delta t \Delta P} \tag{19}$$

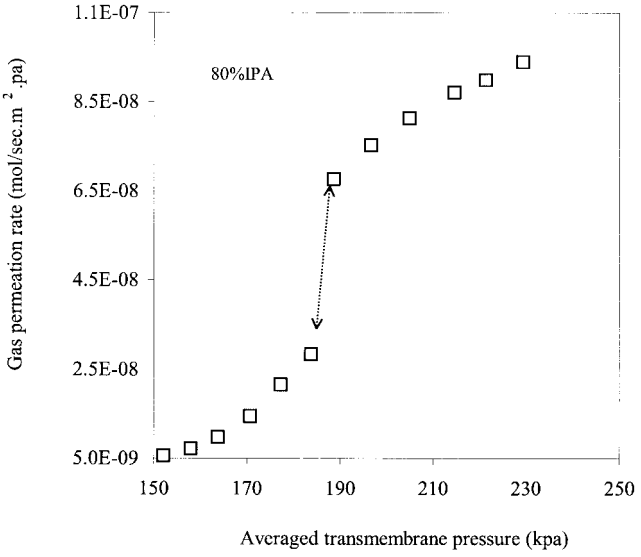

Figure 6. Progressive gas permeation rate of membrane B vs. the averaged pressure.

where V is volume of the gas permeate measured within a time interval Δt, Δp is transmembrane pressure, and A is effective membrane area.

Results and Discussion

Permeation behaviors of wetted membranes

The gas permeation rates of the two MF membranes are plotted against the averaged pressure in Figures 5 and 6. The typical "S-Shape" curves are obtained, implying that the water-filled pores in the wetted membranes are gradually opened by the transmembrane pressure. The pressure increment set in this experiment is very small (around 2 psi) so that the representative information on pore statistics can be revealed. Compared with membrane A, as illustrated in Figure 5, the gas permeation rate of membrane B, as shown in Figure 6, increases less "uniformly," and a big leap can be observed when the averaged pressure varies from 185~190 kpa psi. It can also be estimated that more than one-third of the "total permeation rate" of membrane B was represented by the leap, and, most probably, the pore-size distribution of membrane B will center at the pore size corresponding to this pressure range. A smaller leap can also be observed in Figure 6, however, the relative contribution is not that significant, implying that the pore-size distribution of membrane A is less sharp than that of membrane B.

Incremental pore-size distribution in terms of porosity ($\varepsilon - r$)

The incremental pore-size distributions of membranes A and B are illustrated in Figures 7 and 8, respectively. Membrane A has a relatively dispersed distribution as predicted previously, the statistically important pore radii of membrane A are in the range of 0.3–1.5 μm. The peak porosity is a little bit more than 20%, shared by the group of the pores with a nominal radius of 0.53 μm. It can also be found in Figure 7 that the porosity of membrane A is largely represented by the pores ranging from 0.38–0.48 μm, which account for nearly 40% of the total

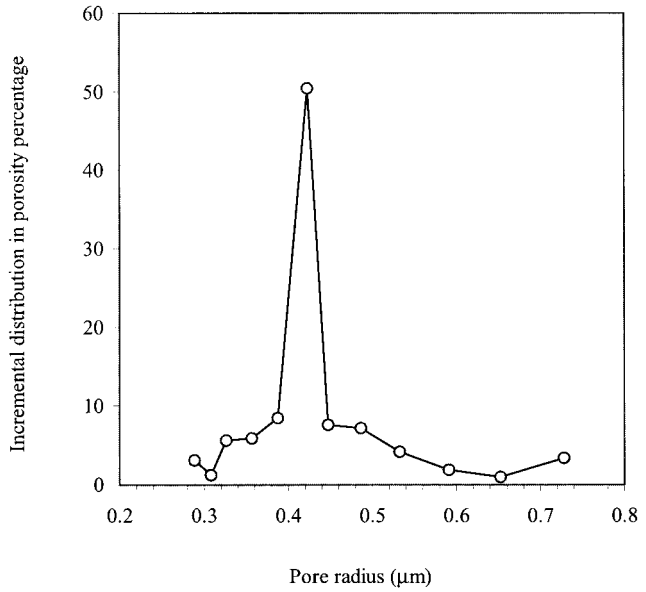

Figure 8. Incremental pore-size distribution of membrane B.

porosity as demonstrated in the accumulative pore-size distribution illustrated in Figure 9. Membrane B shows a very sharp pore-size distribution, which can be essentially characterized by a normal distribution centered at 0.42 μm. One eminent characteristic of the distribution is that more than 50% of the total porosity goes to the single group of pores (the peak pore, 0.42 μm). This sharp pore-size distribution justifies an interesting observation in the experiment. When the upstream pressure was set close to the bursting pressure of the peak pores, the gas flow for membrane B kept going up rather than reach a constant (the steady-state flow) in a short transition time period. It took more than 3 min for the membrane to achieve its

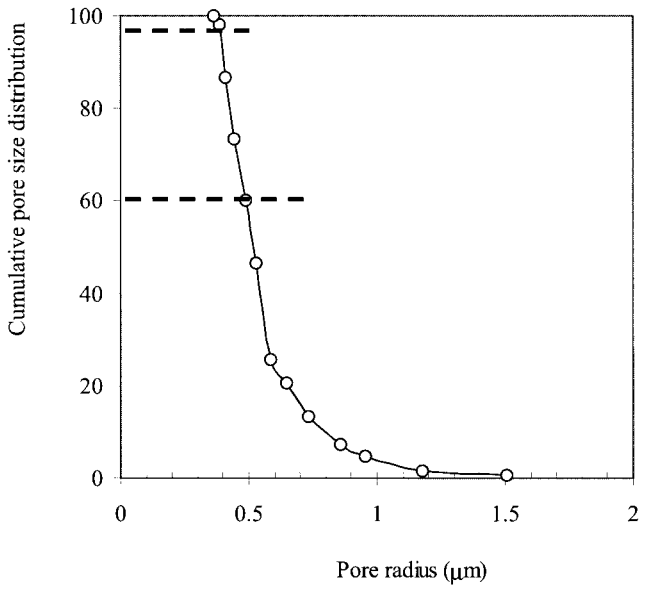

Figure 9. Cumulative pore-size distribution of membrane A.

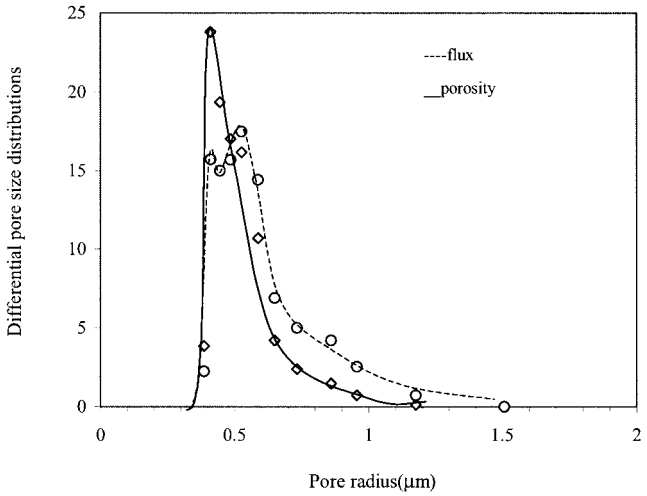

Figure 10. Differential pore-size distribution of membrane A.

constant flow rate. This phenomenon can be interpreted by the "continuous" subdistribution of pore size inside the peak pore group. Considering that 50% of the total porosity is packed in this narrow gap of pore size, the individual pore-size difference in this pore group must be very small, and a very slight fluctuation in transmembrane pressure can, therefore, get a quite number of pores opened. It is true to some extent that the increment of pressure in this situation is set more by the membrane itself than by the experimenter. This also poises a problem that the fine determination of pore-size distributions can be very challenging, particularly in cases where sharp distributions exist.

Differential pore-size distributions [(dε/dr) − −r] and [(dεr²/dr) − −r]

The differential pore-size distributions of membranes A and B are depicted in Figures 10 and 11, the distribution in terms of

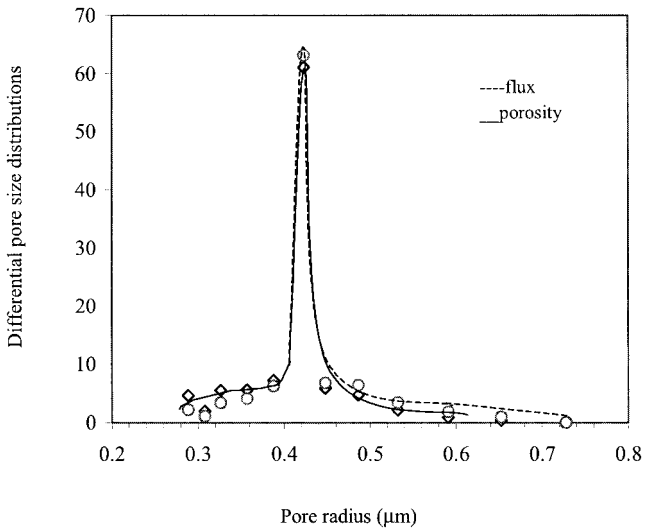

Figure 11. Differential pore-size distribution of membrane B.

porosity $[(d\varepsilon/dr) - -r]$ is denoted by the solid line, and distribution in terms of flux $[(d\varepsilon r^2/dr) - -r]$ denoted by the dashed line. For membrane A, these two types of distributions differ from each other in many ways. Two peaks are observed in the differential distribution in flux percentage, and the pore size corresponding to the maximal percentage shifted from 0.41 μm in the distribution of $[(d\varepsilon/dr) - -r]$ to 0.53 μm in $[(d\varepsilon r^2/dr) - -r]$, and the peak probability is reduced from about 24% to about 17%. According to the definition of the pore-size distribution of $[(d\varepsilon r^2/dr) - -r]$, the probability is proportional to the square of pore radius. As a result, the probability of a larger pore will be assigned with a bigger weight (r_i^2); this is why increased probabilities compared with that in $[(d\varepsilon/dr) - -r]$ is imparted to larger pores, and decreased probability is assigned to smaller pores. A similar relationship can be found in Figure 11 except that no noticeable shift happens to membrane B. As is known, membrane B has a very sharp distribution, and changes in definitions of pore-size distributions cannot result in significant variations.

Pore-size distributions based on transition regime and Hagen-Poiseuille regime

Theoretical analysis shows that Knudsen diffusion in capillary pores can be reasonably ignored when the ratio of pore radius to mean free path is larger than 10. It has been specified in the Experimental section that the contact angle of water on the surface of the sulfonated poly(ether ether ketone) is 58.2°; therefore, the effective surface tension in this case is 36.4 mJ/m^2. Take membrane A, whose pore sizes range from 0.3–1.5 μm, for example, according to Figure 2, when pore radius is larger than 0.3 μm, but less than 0.5 μm, the fraction of Knudsen diffusion is 6%–5%, and when pore radius is bigger than 0.5 μm, the fraction of Knudsen diffusion is less than 5%, meaning that by sacrificing some accuracy, the pore-size distributions of membrane A can be estimated by the approximated model based on Hagen-Poiseuille regime. The differential pore-size distributions based on transitional regime (donated by solid lines) and Hagen-Poiseuille regime (donated by dashed lines) are illustrated in Figures 12 and 13. It can be seen in Figure 12 that the probabilities of larger pores (relative to the peak pores) are overestimated by Hagen-Poiseuille regime. The error introduced by the approximation treatment increases with a decrease in pore size. Since the fractions of Knudsen diffusion in smaller pores are relatively higher, bigger errors are, thus, brought to the probabilities of smaller pores (relative to the peak pores), which is also underestimated. All these show that the ratio of the pore size to the mean free path is a useful and an effective parameter in judging the working regime of gas transport through various membrane pores. Reliable information on pore-size distributions cannot be obtained by approximate model unless pore sizes of the membranes are large enough (such as larger than 0.5 μm in this case). Generally speaking, the universal model based on the transport equation of slip flow should always be employed if there is no priori analysis conducted to make sure which regime dominates the gas transport in the membrane. This criterion is supported by Figure 13, where two peaks are observed in the pore-size distribution estimated by the universal model, however, such information is completely erased in the pore-size distribution estimated by the approximate model.

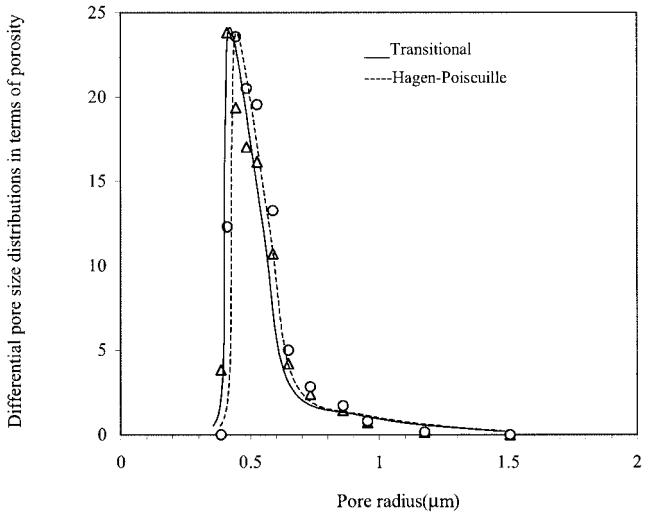

Figure 12. Differential pore-size distributions of membrane B in porosity percentage estimated based on slip flow regime and Hagen-Poiseuille regime.

Conclusions

Theoretical analysis shows that slip flow dominates gas transport in MF membranes whose pore sizes range from 0.1–10 μm, although Knudsen diffusion in some cases can be suppressed by selecting the right pore-filling liquids, whose effective surface tension must be higher than 72.8 mJ/m^2. A universal mathematical model for estimating pore-size distributions of MF membranes was developed based on the transport equation governing slip flow, and a simplified model was also presented where only Hagen-Poiseuille flow is considered.

The pore-size distributions of two MF membranes were obtained using the universal model and then simplified. Results

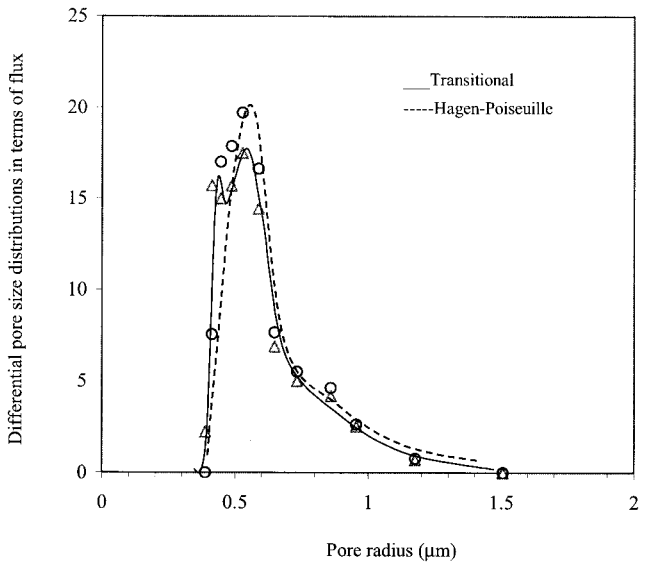

Figure 13. Differential pore-size distributions of membrane A in flux percentage estimated based on slip flow and Hagen-Poiseuille regime.

show that the simplified model overestimates the probabilities of larger pores (relative to the peak pore), and underestimates the probabilities of smaller pores (relative to the peak pores). It is also found that the simplified model cannot disclose some subtle features in pore-size distributions owning to the relatively big errors introduced. For the sake of accuracy in characterizing pore-size distributions of MF membranes, the universal model is strongly recommended.

Acknowledgments

The Natural Sciences and Engineering Research Council (NSERC) of Canada is gratefully acknowledged for funding this research project.

Literature Cited

Baltus, R. E., "Characterization of the Pore Area Distribution in Porous Membranes Using Transport Measurements," *J. Membrane Sci.,* **123**, 165 (1997).

Bechhold, H., M. Schlesinger, K. Silberesen, L. Maier, and W. Nurnberger, "Pore Diameters of Ultrafilters," *Kolloidz.,* **55**, 172 (1931).

Bottino, A., G. Camera-Rodb, G. Capannelli, and S. Munari, "The Formation of Microporous Polyvinylidene Difluoride Membranes by Phase Inversion," *J. Membrane Sci.,* **57**, 1 (1991).

Dollimore, D., and G. R. Heal, "An Improved Method for the Calculations of Pore Size Distributions from Adsorption Data," *J. Appl. Chem.,* **14**, 109 (1964).

Evans, R. B. III, and G. M. Watson, "Gaseous Diffusion in Porous Media. II Effect of Pressure Gradients," *J. Chem. Physics,* **36**, 1894 (1962).

Frommer, M. A., and R. M. Messalem, "Mechanism of Membrane Formation. VI. Convective Flows and Larger Void Formation During Membrane Precipitation," *Ind. Eng. Chem., Prod. Res. Dev.,* **12**, 328 (1973).

Hernandez, A., J. I. Calvo, P. Pradanos, and F. Tejerina, "Pore Size Distributions in Microporous Membranes. A Critical Analysis of the Bubble Point Extended Method," *J. Membrane Sci.,* **112**, 1 (1996).

Honold, E., and E. L. Skau, "Application of Mercury Intrusin Method for Determination of Pore-Size Distribution of Membrane Filters," *Science,* **120**, 805 (1954).

Huang, R. Y. M., P. Shao, C. M. Burns, and X. Feng, "Sulfonation of Poly(ether ether ketone) (PEEK): Kinetic Study and Characterization," *J. Appl. Polym. Sci.,* **82**, 2651 (2001).

Jakobs, E., and W. J. Koros, "Ceramic Membrane Characterization via the Bubble Point Technique," *J. Membrane Sci.,* **124**, 149 (1997).

Kamide, K., and S. Manabe, "Characterization Technique of Straight-through Porous Membranes," *Ultrafiltration Membranes and Applications,* A. R. Cooper, ed., Plenum, New York (1980).

Kang, J. S., K. Y. Kim, and Y. M. Lee, "Preparation of Microporous Chlorinated Poly(vinyl chloride) Membrane in Fabric and the Characterization of their Pore Sizes and Pore-Size Distributions," *J. Appl. Polym. Sci.,* **86**, 1195 (2002).

Kesting, R. E., *Synthetic Polymeric Membranes, A Structural Perspective,* 2nd ed., Wiley, New York (1985).

Kulkarni, S. S., E. W. Funk, N. N. Li, W. S. W. Ho, and K. K. Sirkar, eds., *Membrane Handbook,* Van Nostrand Reinhold, New York (1992).

Lowell, S., and J. E. Shields, *Powder Surface Area and Porosity, Powder Technology Series,* B. Scarlett, ed., Wiley, New York (1987).

Mason, E. A., and A. P. Malinauskas, *Gas Transport in Porous Media: The Dusty-Gas Model,* Elsevier, Amsterdam (1983).

McEaney, B., and T. J. Mays, *Porosity in Carbon,* J. W. Patrick, ed., Edward Arnold, London, pp. 100–101 (1988).

Meyer, K., and P. Klobes, "Comparison between Different Presentations of Pore Size Distribution in Porous Materials," *J. Anal. Chem.,* **363**, 174 (1999).

Mulder, M., *Basic Principles of Membrane Technology,* Kluwer, Dordrecht, Netherlands (1991).

Otani, S., N. Wakao, and J. M. Smith, "II: Diffusion and Flow in Porous Catalysts," *AIChE J.,* **11**, 439 (1965).

Pereira Nunes, S., and K. V. Peinemann, "Ultrafiltration Membranes from PVDF/PMMA Blends," *J. Membrane Sci.,* **77**, 25 (1992).

Present, R. D., *Kinetic Theory of Gases,* McGraw-Hill, New York (1958).

Schofield, R. W., A. G. Fane, and C. J. D. Fell, "Gas and Vapor Transport through Microporous Membranes. I. Knudsen-Poiseuille Transition," *J. Membrane Sci.,* **53**, 159 (1990).

Scott, D. S., and F. A. L. Dullien, "Diffusion of Ideal Gases in Capillaries and Solids," *AIChE J.,* **8**, 113 (1962).

Scott, D. S., and F. A. L. Dullien, "The Flow of Rarefied Gases," *AIChE J.,* **8**, 293 (1962).

Smith, D. M., and D. P. Gallego, *Studies in Surface Science and Catalysis,* K. K. Unger, J. Rouquerol, K. S. W. Sing, and H. Krahl, eds., Elsevier, Amsterdam, Vol. 39, pp. 391–400 (1977).

Wakao, N., S. Otani, and J. M. Smith, "Significance of Pressure Gradients in Porous Materials," *AIChE J.,* **11**, 435 (1965).

Manuscript received Apr. 28, 2003, and revision received Jun. 19, 2003.